Proc. Vth International Workshop, Advances in Signal Processing for Non Destructive Evaluation of Materials
Québec City (Canada),2-4 Aug. 2005. © X. Maldague ed., É. du CAO (2006), ISBN 2-9809199-0-X

# Detection of subsurface inclusions by magnetic flux density measurements using a fluxgate gradiometer

by Hector Carreon

*Instituto de Investigaciones Metalúrgicas, Universidad Michoacana, Edif."U" Ciudad Universitaria, Morelia, Mich. Mexico 58000-888*

**Abstract**

A comparison between published analytical results with measured experimental results of the magnetic field produced by thermoelectric currents of subsurface semi-spherical pure tin inclusions embedded in a copper bar under the influence of an external heating and cooling into the specimen is presented. The experimental magnetic flux density measurements show a reasonable agreement as compared to analytical data with the exception of the intrinsic material background magnetic signal that affected deeply the detectability of subtle imperfections in noncontacting thermoelectric measurements.

**Keywords:** thermoelectric NDE, magnetic detection, subsurface inclusions

## 1. Introduction

In general the conventional thermoelectric technique monitoring the thermoelectric power of conductor materials, is sensitive to small changes caused by material imperfections. In order to apply the thermoelectric technique for QNDE material characterization, a conductor with well-defined properties (reference probe) and a known temperature difference along it, is used to evaluate the properties given by changes in the thermoelectric power of a second conductor (test sample). However several effects can affect these changes in the thermoelectric power of the test sample. The most important effects affecting the thermoelectric measurements are those associated with volumetric and contact effects. The volumetric effect is close related to the thermoelectricity phenomena by the kinetics of the diffusion of electrons throughout the material. This effect is mainly affected by chemical composition, anisotropy, hardening, texture etc. The contact effects are related to the imperfect contact between the test sample and the reference probe [1]. On the other hand, the new noncontacting thermoelectric method uses the surrounding intact material as the reference probe; thus provides perfect interface between the region to be tested and the surrounding material. In the self-referencing thermoelectric method the material imperfections naturally form thermocouples in the specimen itself and, in the presence of an externally induced temperature gradient, these thermocouples produce thermoelectric currents around the imperfections that can be detected bias the magnetic flux density B by magnetic sensors from a significant lift-off distance between the tip of the sensor and the material surface imperfection. Even when the material imperfections are rather deep below the surface [2,3]. Figure 1 shows a schematic diagram of the noncontacting thermoelectric measurements process in the presence of material imperfections as most often used in nondestructive materials characterization. In this paper, we review experimental results which demonstrate that the analytical predictions for the case of subsurface semi-spherical inclusions in a homogeneous host material under external thermal excitation truthfully captures the main features of the thermoelectrically generated magnetic field and predicts its magnitude over a wide range of subsurface inclusion sizes embedded in a copper bar and also it shows experimental evidence of the negative effect produced by macrostructural features in thermoelectric NDE especially when the material imperfections (inclusions) are rather deep below the surface. First, we present a review of the analytical model of Reference [4], and then we will proceed by describing the experimental procedure and, finally, discuss the experimental results and compare them to the analytical predictions.

## 2. Analytical model

In order to illustrate the analytical magnetic field distributions of fully embedded hidden inclusions with the center of a spherical inclusion lies below the surface at a depth *d*, that is deeper than its radius $a$. We present numerical results obtained by the analytical model described in Ref. [4], in which all spatial coordinates are normalized to the radius of the spherical inclusion as $\boldsymbol{\xi} = \mathbf{x} / a$. The magnetic field is also written in a normalized form as $\mathbf{H} = H_0 \mathbf{F}(\boldsymbol{\xi})$. Finally, the estimation of the absolute strength of the magnetic field is written as $H_0 = -a\nabla T \sigma (S' - S)\Gamma$ where $a$ is the radius of the inclusion, $\nabla T$ is the externally induced temperature gradient, $\sigma$ is the thermal conductivity of the host, $S_{SR} = S' - S$ is the relative thermoelectric power of the inclusion with respect to the host, $\Gamma$ is a normalized contrast coefficient and $\mathbf{F}(\boldsymbol{\xi})$ is a universal spatial distribution function for all spherical inclusions. Figure 2 shows the two-dimensional distributions of the normal component of the normalized magnetic field for a subsurface spherical inclusion at two different depth distances *d* = $a$ and *d* = $2a$ respectively. The magnetic field to be detected rapidly decreases with the depth of the inclusion. The normal component drops from $F_1 \approx 0.4$ at *d* =$a$ to as low as $F_1 \approx 0.164$ at *d* =$2a$. The distribution is obviously very similar to that of a surface-breaking inclusion, that was previously published by author *et al*., except that the bipolar lobes are more extended and rounded and accordingly the peak values are slightly reduced. The magnetic field distribution became significantly weaker and wider as the inclusion depth distance increase. The thermoelectric currents flow in opposite directions along two loops on the opposite sides of the inclusion depends on the heat flux direction as predicted by Figure 1.

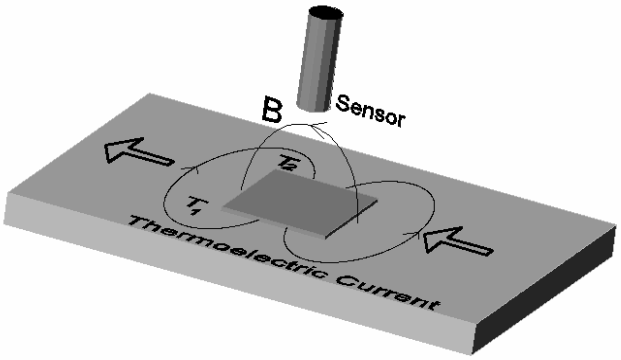


*Figure 1* schematic diagram of noncontacting thermoelectric detection of material imperfections by magnetic monitoring of thermoelectric currents.

## 3. Experimental method

In order to compare the magnitude, over a range of inclusion sizes and lift-off distances, of the analytical magnetic field produced by subsurface semi-spherical inclusions embedded in a homogeneous host material under external thermal excitation with respect to the experimental magnetic field. First, we prepared the specimen, for this reason, it was selected a plate of copper as the host medium and tin as the embedded inclusion. The copper bar (specimen) was cut from a copper plate with a 12.7 mm × 38.1 mm × 500 mm dimensions. The copper specimen was milled to obtain different semispherical holes ranging from 12.7 to 3.18 mm at the specimen surface with a distance of 75 mm between them in order to avoid interference between their individual magnetic fields. The depth of each hole was the same as its radius. Then the specimen was heated to approximately ≈ +300 °C

and filled the holes with molten pure tin in order to obtain surface semi-spherical inclusions embedded in the copper bar. Finally, the specimen was cooled down and milled the surface flat. The 12.7 mm-thick copper bar with the several embedded surface breaking tin inclusions was turned upside down so that the surface-breaking inclusions were at the bottom simulating subsurface semi-spherical inclusions. The copper specimen was mounted and equipped by heater exchangers in order to heat and cool it simultaneously by running water at temperature of $\approx +45°C$ and $\approx +10°C$, respectively. All the assembly was mounted on a translation table for scanning. Since the temperature of the cold and hot water in the laboratory inevitably varied by a couple degrees, the actual temperature difference between the ends of the bar was monitored during the magnetic flux density measurements. The temperature gradient was $\approx 0.7°C/cm$, which is more than sufficient to produce detectable magnetic signals in high-conductivity materials like copper and tin. The magnetic flux density measurements of the different diameter subsurface semi-spherical tin inclusions were detected by a fluxgate (magnetometer) sensor in both temperature gradient directions as shown in Figure 3.

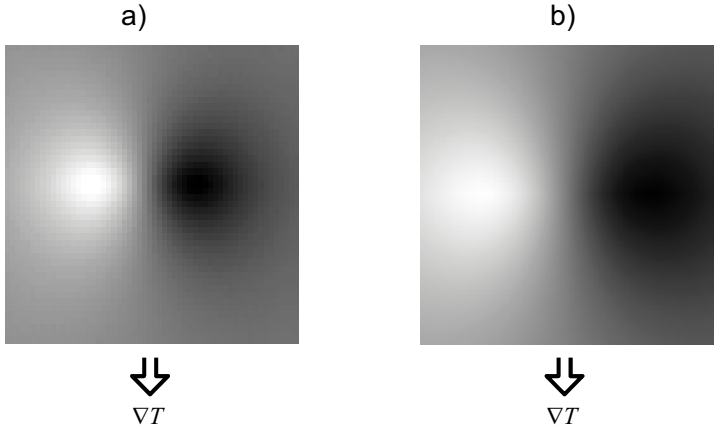


*Figure 2* two-dimensional distributions of the normal component of the normalized magnetic field for a subsurface spherical inclusion at two different depths a) $d = a$ and b) $d = 2a$ respectively.

To calculate a quantitative comparison to the analytical predictions, the relevant physical properties of pure copper and tin were taken from standard book references with the exception of the absolute thermoelectric power of tin inclusion at room temperature, which was measured by a Koslow TE-3000 thermoelectric instrument on the largest inclusion itself since it was found to be significantly affected by the sample preparation process (melting and recrystallization) [5]. The specimen was scanned with a 3 axis magnetic field sensor (Mag-03 Bartington) that has a sensitivity of $10\mu T/V$. This fluxgate (magnetometer) sensor has three sensing elements individually potted. The dimension of the sensing element of each sensor (fluxgate) is a cylinder of 15 mm length $\times$ 1 mm radius independently encapsulated with reinforced epoxy with dimensions of $8\times8\times25$ mm. In the experiment, only a pair of fluxgate sensors configurated in a gradiometric arrangement was used to detect the magnetic flux density from the copper specimen. The primary sensor closer to the specimen detects a much stronger signal from the inclusion than the secondary sensor further away, while the two sensors present the same sensitivity for sources at large distances [5]. The geometric center of the fluxgate is approximately 12.5 mm below the tip of the epoxy-encapsulated case, i.e., the $g$ = 2 mm apparent lift-off corresponds to a much larger 14.5-mm actual lift-off distance. The baseline distance $b$ and the inclusion depth distance $d$ were chosen to be 28.6 mm and 11.5 mm respectively in our case as shown in Figure 3. The baseline distance and inclusion depth optimization depend on the spatial distribution of the magnetic field to be measured [4,5]. The fluxgate (gradiometer) sensor was located above the centerline of each subsurface inclusion. The magnetic signal produced by the different subsurface tin

inclusion diameters was detected by laterally (normal to the heat flux) scanning the copper specimen at a speed of 20 mm/s.

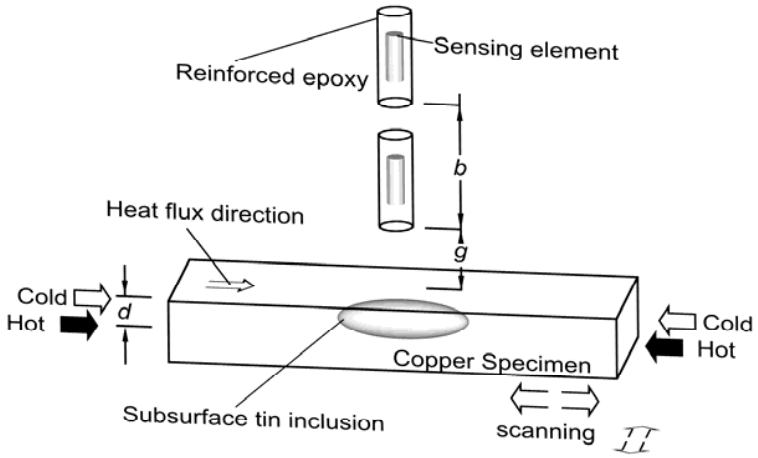


*Figure 3* schematic diagram of the experimental set up.

## 4. Experimental results

Figure 4 shows the magnetic images recorded from two subsurface semi-spherical tin inclusions. These measurements were taken from the copper specimen of 12.7 mm-thick copper bar turned upside down so that the surface-breaking inclusions were at the bottom simulating subsurface inclusions with a depth distance given by *d*. These pictures were taken at 2 mm distance above the copper specimen surface. This apparent lift-off distance is the distance between the tip of the fluxgate magnetometer and the copper specimen surface. However, the sensing element of the fluxgate magnetometer is a 15-mm-long ferromagnetic rod buried at an average distance of 12.5 mm below the surface of the probe, therefore, for the purposes of comparison with the analytical predictions of the magnetic flux density, this experimental configuration corresponds to a much larger 14.5 mm lift-off. The measured magnetic field distributions are very similar in shape to the analytical predictions previously shown in Figure 2. As we expected, the characteristic main bi-polar lobes change sign when the direction of the temperature gradient in the specimen is reversed. These main lobes get wider and the magnitude of the magnetic flux decreases when the lift-off distance is increased. Also the magnetic field became significantly weaker and the spatial distribution of the field revealed some distortions. Beside the previously observed two main lobes, two weaker secondary lobes could also be observed. This particular feature is not predicted by the simple analytical model and is most probably associated with the finite width (12.7 mm) of the copper bar, which is expected to affect the measurements much more when the inclusion is rather deep below the surface due to the fact that the intrinsic material background signature affected the POD of subtle material flaws in the noncontacting thermoelectric technique for QNDE material characterization. Finally, Figure 5 shows how the peak-to-peak magnetic flux density changes with the lift-off distance between 1 and 8 mm for five inclusions of different diameters between 12.7 and 3.18 mm. The solid lines represent the analytical predictions while the solid points represent the experimental results based on the material properties listed. The lift-off distance was corrected for the depth of the sensing element below the surface of the probe and also for the inclusion depth distance, but no other adjustments were made. The results are plotted in Figure 5 that compares the experimentally measured and theoretically predicted magnetic flux densities for different diameters and lift-off distances. Considering the rather crude approximations used in the theoretical model, the large

number of independent material parameters involved in the phenomenon and their inherent uncertainties, and the potential experimental errors associated with the measurements, the agreement between experimental results and analytical predictions over a range of more than two orders of magnitude is so good.

a) 6.35 mm-diameter subsurface semi-spherical inclusion, B ≈ 2.3 nT

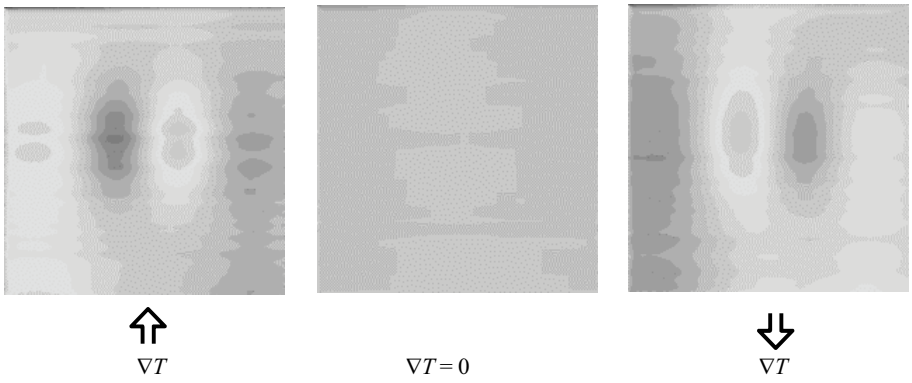


b) 9.53 mm-diameter subsurface semi-spherical inclusion, B ≈ 8.6 nT

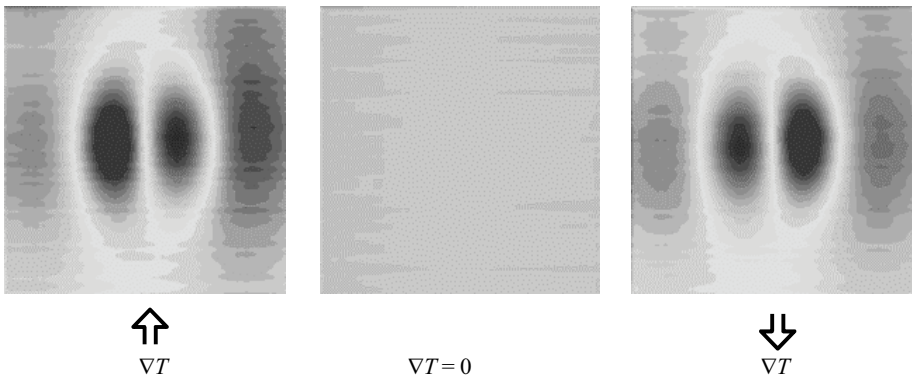


*Figure 4* magnetic images of subsurface semi-spherical tin inclusions ($\nabla T \approx 0.7$ $^{O}$C/cm, 2 mm lift-off distance, 76.2 mm × 76.2 mm scanning dimension, the peak magnetic flux density B is indicated for comparison).

## 5. Conclusions

In conclusion, the preliminary measurements clearly demonstrate that the thermoelectric technique for QNDE material characterization is a very powerful one. It should be stressed that it is able to detect inclusions, which are located below the surface. However, this new technique requires a substantial research effort to establish a solid scientific foundation for successful future applications. This goal can be reached by conducting a coordinated theoretical and experimental study of the feasibility of thermoelectric detection and characterization of inclusions and other types of flaws in metals. The results also indicate that the detection sensitivity of the noncontacting thermoelectric method can be limited by unwanted background signal that interferes with, and often conceals, the inclusion signals to be detected. The main sources of such adverse background signals in thermoelectric NDE are the intrinsic variations of the material properties of the specimen to be inspected.

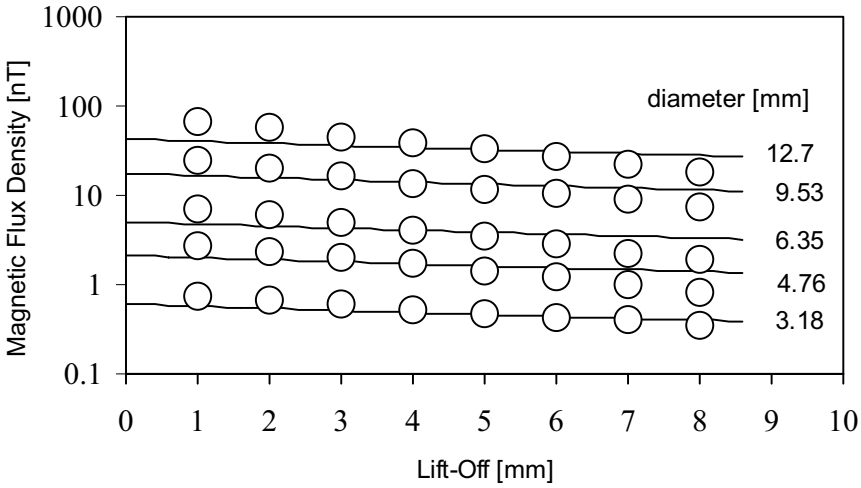


*Figure 5* comparison between the experimentally measured and theoretically predicted peak-to-peak magnetic flux densities plotted as functions of the lift-off distance for subsurface semi-spherical tin inclusions in copper.

## REFERENCES

[1]FULTON (J.), WINCHESKI (B.), and NAMKUNG (M.).- *Automed weld characterization using the thermoelectric method*, Nondestructive Evaluation Science Branch, NASA 1993; Langley Research Center.

[2]TAVRIN (Y.), KRIVOY (G.), HINKEN (J.) and KALLMEYER (J.).- *A thermoelectric method to detect weak local structural changes and inclusions in metal part.* in Review of Progress in QNDE, Vol. 20. AIP, 2001. p. 1710-1716.

[3]. CARREON (H.), LAKSHMINARAYAN (B.) and NAGY (P.*)*.- *Thermoelectric background signature due to the presence of material property gradients.* in Review of Progress in QNDE, Vol. 23. AIP, 2004. p. 445-452

[4] NAGY (P.) and NAYFEH (A.).- *On the thermoelectric magnetic field of spherical and cylindrical inclusions.* Journal of Applied Physics Vol. 87, 2000, p. 7481-7490.

[5] CARREON (H.), NAGY (P.) and NAYFEH (A.).- *Thermoelectric detection of spherical tin inclusions in copper by magnetic sensing.* Journal of Applied Physics Vol. 88, 2000, p. 6495-6500.

[6] NAYFEH (A.), CARREON (H.) and NAGY (P.).- *Role of anisotropy in noncontacting thermoelectric materials characterization.* Journal of Applied Physics Vol. 91, 2002, p.225-231.